

Study of dynamic heterogeneity of an active particle system

Huai Ding, Huijun Jiang, and Zhonghuai Hou*

*Department of Chemical Physics and Hefei National Laboratory for Physical Sciences at Microscales,
University of Science and Technology of China, Hefei, Anhui 230026, China*

(Received 14 February 2017; published 24 May 2017)

We have studied spatial and temporal dynamic heterogeneity (DH) in a system of hard-sphere particles, subjected to active forces with constant amplitude and random direction determined by rotational diffusion with correlation time τ . We have used a variety of observables to characterize the DH behavior, including the deviation from standard Stokes-Einstein (SE) relation, a non-Gaussian parameter $\alpha_2(\Delta t)$ for the distribution of particle displacement within a certain time interval Δt , a four-point susceptibility $\chi_4(\Delta t, \Delta L)$ for the correlation in dynamics between any two points in space separated by distance ΔL within some time window Δt , and a vector spatial-temporal correlation function $S_{\text{vec}}(R, \Delta t)$ for vector displacements within time interval Δt of particle pairs originally separated by R . By mapping the particle motion into a continuous-time random walk with constant jump length, we can obtain the average waiting time $\langle t_x \rangle \propto D_s^{-1}$ and persistence time $\langle t_p \rangle \propto \eta$, with D_s the self-diffusion coefficient and η the shear viscosity, such that the observable $\lambda = \langle t_p \rangle / \langle t_x \rangle \propto D_s \eta$ can be calculated as a function of the control parameter τ to show how it deviates from its SE value λ_0 . Interestingly, we find λ/λ_0 shows a nonmonotonic behavior for large volume fraction ϕ_a , wherein λ/λ_0 undergoes a minimum at a certain intermediate value of τ , indicating that both small and large particle activity may lead to strong DH. Such a reentrance phenomenon is further demonstrated in terms of the non-Gaussian parameters α_2 , four-point susceptibility χ_4 , and vector spatiotemporal correlation functions S_{vec} , respectively. Detail analysis shows that it is the competition between the dual roles of particle activity, namely, activity-induced higher effective temperature and activity-induced clustering, that leads to such nontrivial nonmonotonic behaviors. In addition, we find that DH may also show a maximum level at an intermediate value of ϕ_a if τ is large enough, implying that a more crowded system may be less heterogeneous than a less crowded one for a system with high particle activity.

DOI: [10.1103/PhysRevE.95.052608](https://doi.org/10.1103/PhysRevE.95.052608)

I. INTRODUCTION

The phenomenon of dynamic heterogeneity (DH), which relates to the spatiotemporal fluctuation of the system [1], frequently exists in supercooled liquid [2–4], highly crowded colloid systems [5,6], and cellular environment [7]. Basically, DH describes the phenomenon in such systems that some regions of sample exhibit faster dynamics than the rest, and over time these mobile regions appear and disappear throughout the system. The study of DH originally stemmed from the explanation of the nonexponentiality of relaxation processes in supercooled liquids [4], related to the existence of a broad relaxation spectrum. It was understood that a multiple superposition of slow and fast relaxators [8,9] in different regions gives rise to highly nonexponential relaxation behavior of intermediate scattering functions. The motion of particles within the faster mobile region is cooperative, namely, the fast relaxators are correlated over large distances [10], which can make the system return back to the ergodic state even rest of particles were completely trapped with a very slow relaxation in the cages formed by the crowding environment. The coexistence of faster and slower particles also results in an exponential rather than Gaussian tails of self-part of the van Hove function [1,11].

Another influential phenomenon that was early related to the existence of DH is the decoupling of self-diffusion (D_s) and viscosity (η) [12,13]. Since structural relaxation is usually associated with rotational diffusion of particles,

such a decoupling between diffusion and viscosity is also reflected by the decoupling between translation and rotational diffusion in complex fluids [14,15]. For a high-temperature homogeneous liquid, self-diffusion and viscosity are related by the well-known Stokes-Einstein (SE) relation [13], $D_s \eta / T = \text{const}$ with T being the temperature. Physically, the SE means that two different measures of the relaxation times d^2/D_s and $d^3 \eta / T$ lead to the same time scale up to a constant factor, where d denotes the particle diameter. Nevertheless, for a system with DH such as supercooled liquid, this SE relation may break down, and it is commonly found that D_s^{-1} does not increase as fast as η/T so that $D_s \eta / T$ may be two to three orders of magnitude as compared to its SE value. Indeed, different observables probe differently the underlying distribution of relaxation times. For a system with fast and low regions of particles, the self-diffusion coefficient of a tagged tracer particle is dominated by the more mobile particles, whereas the viscosity or other measures of structural relaxation probe the time scale needed for every particle to move and are contributed mainly by those slow particles. Therefore, the deviation from SE relation can be used as an important factor to measure the DH property of a system. We note that a variety of experimental techniques, such as multidimensional nuclear magnetic resonance [16,17], dielectric and magnetic hole burning [18–20], deep photo bleaching [21,22], etc., have been developed in recent years to study DH behaviors with particular range of accessible time and temperature scales. Molecular dynamics simulations have also been widely used for studying DH feature of a variety of model systems above the onset temperature of glass transition predicted by mode coupling theory [23,24].

*Corresponding author: hzhjlj@ustc.edu.cn

Whereas the studies of DH in space and time provide a significant step towards understanding the relation between the macroscopic properties of soft condensed matter and the microscopic molecular mechanisms involved [1,12], most of the works so far have mainly focused on the descriptions of equilibrium glassy liquids. On the other hand, very recently, the collective behaviors of *active* particles have gained extensive research attentions [10,25–33]. The particles are subjected to some kind of self-propulsion force which is not balanced by the thermal noise, pushing the system out of equilibrium. There have been a variety of models for active particle systems, including the active Brownian particle model [27,34] wherein the self-propulsion force is constant in amplitude but changes direction randomly via rotational diffusion, and the active colored noise model wherein the self-propulsion force is described by an Ornstein-Uhlenbeck (OU) stochastic process [35,36], for instances. It has been shown that particle activity, quantified by amplitude of the propulsion force as well as the persistence time of its directional motion, strongly influences the system dynamics. A wealth of interesting nonequilibrium phenomena have been reported, such as active swarming, large scale vortex formation [29,30,37,38], phase separation [28,31,34,39–41], etc., both experimentally and theoretically. Recently, the dynamics of dense assemblies of self-propelled particles around glass transition has been a new trend in this field. Experiments on crowded systems of active colloids and active cells show dynamic features such as jamming and dynamic arrest that are very similar to those observed in glassy materials [7,42]. Computer simulations demonstrated that nonequilibrium glass transition or dynamic arrest behavior does occur in a dense suspension of self-propelled hard spheres, where the critical density for glass transition shifts to larger value with increasing activity [10,27]. Therefore, one would expect that DH should also be an important feature in such nonequilibrium condensed systems. Very recently, Flenner *et al.* [43] had performed a detailed study of the nonequilibrium glassy dynamics of mixture of athermal self-propelled particles, wherein the authors had paid some attention on the DH feature by investigating the behavior of a dynamic susceptibility based on the fluctuations of the real part of the microscopic self-intermediate scatter function. Nevertheless, the interesting topic regarding how particle activity would affect the spatial and temporal DH behavior of active particles system still deserves a systematic understanding.

Motivated by this, in this paper, we have studied the spatial and temporal dynamic behaviors of an active hard-sphere particle system, paying particular attention on how the particle activity would influence DH features. The particles are subjected to an external active force with constant amplitude f_0 , of which the direction stochastically changes via rotational diffusion with correlation time $\tau = \frac{1}{2D_r}$, where D_r is the rotational diffusion coefficient. For fixed value of f_0 , the parameter τ can be used to characterize the particle activity. We have studied how the DH property depends on particle activity by using a couple of different measures. First, we investigate how the normal SE is violated with the variation of the particle activity. This is done by mapping the particle motion into a continuous-time random walk (CTRW) with constant jump length, wherein one can obtain the average

waiting time $\langle t_x \rangle$ between adjacent jump events and the averaging persistence time $\langle t_p \rangle$ before the next jump event. The observable $\lambda = \langle t_p \rangle / \langle t_x \rangle$, which is assumed to be proportional to $D_s \eta$, is then calculated as a function of the control parameter τ to show how it deviates from its SE value λ_0 . Second, we study how the distribution of particle displacement within a certain time interval Δt would deviate from Gaussian, which is manifested by a non-Gaussian parameter $\alpha_2(\Delta t)$. For a system with strong DH, a population of particles may move much faster than else such that $\alpha_2(\Delta t)$ shows large deviation from zero. The dependencies of α_2 on Δt for different volume fraction and particle activity are then presented to demonstrate the DH feature at different time scales. In addition, we have also investigated temporal heterogeneity of the dynamics by using the four-point susceptibility $\chi_4(\Delta t, \Delta L)$ which measures the correlation in dynamics between any two points in space separated by distance ΔL within some time window Δt , and spatial DH feature of the system by using the vector spatial-temporal correlation function $S_{\text{vec}}(R, \Delta t)$, which characterizes correlations in the vector displacements within time interval Δt of particle pairs originally separated by R . Consequently, we find that the DH features depend strongly on τ as well as the volume fraction ϕ_a . While λ/λ_0 may show weak dependence on τ for small volume fraction of particles, an interesting reentrance behavior is found for large ϕ_a , wherein λ/λ_0 shows an apparent valley region at intermediate values of τ . Such a nonmonotonic dependence indicates that the dense system becomes most homogeneous for an optimal value of particle activity, while small or large activity may both lead to strong heterogeneity. Such a reentrance behavior is further demonstrated and analyzed in terms of $\alpha_2(\Delta t)$, $\chi_4(\Delta t, \Delta L)$, and $S_{\text{vec}}(R, \Delta t)$, respectively. Furthermore, another interesting nonmonotonic behavior for large particle activity is also found, i.e., DH level shows a maximum at an intermediate value of ϕ_a , implying that a more crowded system with larger ϕ_a may be less heterogeneous than a less crowded system, which sounds counterintuitive at the first glance. All these nontrivial findings clearly demonstrate the intriguing roles of particle activity on DH features of the system.

The paper is organized as follows. In Sec. II, we present descriptions of the model and the methods used to characterize the DH behavior. Detailed results are given by Sec. III, followed by a short conclusion remark in Sec. IV.

II. MODEL AND METHOD

A. Model of self-propelled particles

Here, we consider a two-dimensional (2D) system of N active hard-sphere particles with diameter d . Each particle is subjected to a self-propulsion force with constant amplitude f_0 whereas its direction changes via rotational diffusion. The particles move in a viscous medium that is characterized by the friction coefficient of a single particle γ . The dynamics of the particles is described by [34]

$$\begin{aligned} \dot{\mathbf{r}}_i &= \gamma^{-1} f_0 \mathbf{p}_i + \boldsymbol{\xi}_i(t), \\ \dot{\mathbf{p}}_i &= \boldsymbol{\zeta}_i \times \mathbf{p}_i, \end{aligned} \quad (1)$$

where \mathbf{r}_i is the position vector of particle i and \mathbf{p}_i denotes the unit direction vector of its self-propulsion force. ξ_i and ζ_i are Gaussian white noises with zero mean and have time correlations $\langle \xi_i(t)\xi_j(t') \rangle = 2D_0\mathbf{1}\delta_{ij}\delta(t-t')$ and $\langle \zeta_i(t)\zeta_j(t') \rangle = 2D_r\mathbf{1}\delta_{ij}\delta(t-t')$, respectively, where D_0 and D_r are the translational and rotational diffusion coefficients and $\mathbf{1}$ is the unit tensor. One may refer to Eq. (1) as the rotational diffusion active Brownian particle model [36]. In the long time limit, the particle will show normal-diffusion behavior with diffusion coefficient $D_0 + \frac{f_0^2}{6\gamma^2 D_r} = D_0 + \frac{f_0^2\tau}{3\gamma^2}$, corresponding to a higher effective temperature $T_{\text{eff}} = T(1 + \frac{f_0^2\tau}{3k_B T\gamma})$ with k_B the Boltzmann constant.

One notes that, for the above model, the active force subjected to the particle depends not only on the driven speed $v_0 = \gamma^{-1}f_0$, but also on the persistence time of the driven direction given by $\tau = (2D_r)^{-1}$. Actually, after averaging over the rotational degree of freedom, \mathbf{p}_i can be approximated by a color noise with autocorrelation function $\frac{1}{3}e^{-|t-t'|/\tau}$ [34]. For a spherical particle in normal fluids, the translational and rotational diffusion may be coupled, such that $D_r = 3D_0/d^2$ and $\tau = d^2/D_0$ with d to be the particle diameter. More generally, however, D_0 and D_r can be decoupled and one can choose D_0 and D_r as independent parameters. In this work, we will fix the values of D_0 and d which can be adsorbed into dimensionless units. Our main motivation is to investigate the effect of particle activity on the collective DH behaviors. To this end, we simply fix the value v_0 and choose τ as a free parameter. The case when one fixes τ with changing v_0 leads to similar main results.

B. Violation of SE relation

In general, a dynamically heterogeneous system may show many specific features that are quite different from a dynamically homogeneous one. As already mentioned in the Introduction, for a homogeneous system, the long time diffusion coefficient D_s of a tagged particle and the macroscopic shear viscosity η of the system should obey the famous SE relation $D_s\eta/T = \text{const}$ [13]. Nevertheless, for a system with DH, $D_s\eta$ may deviate apparently from a constant value. Therefore, it is convenient for us to investigate how $D_s\eta$ changes with τ to address the issue how the particle activity would influence the DH property. While one may directly calculate the long time diffusion coefficient and viscosity by direct simulations, here we adopt a simpler method introduced in Ref. [44] by mapping the particle motions to a continuous-time random walk (CTRW). This mapping is done by measuring the times of single-particle events (exchange events) that occur when a particle moves a distance d_0 from its initial position, corresponding to a CTRW where the jump length is fixed. Two times can be extracted from the particle trajectory: one is the random walk waiting time t_x between two exchange events, and the other is the persistence time t_p that starts at a random time and ends at the subsequent exchange event. Generally, d_0 is a characteristic length sufficient for the particle motion to be diffusive and often set to be the first peak in the pair distribution function. Here, we just set $d_0 = d$ due to the hard-core potential. In Fig. 1, a typical trajectory of the particle is shown (left) and the definitions of t_x and t_p

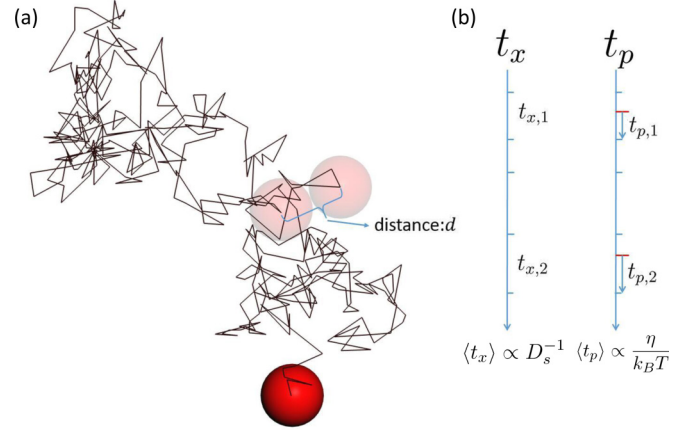


FIG. 1. (a) Typical trajectory of the active particle, d is a characteristic length which equals to diameter of sphere. (b) Illustrations of exchange times t_x and persistence times t_p for an arbitrary particle.

are also illustrated (right). According to Ref. [44], the average exchange time $\langle t_x \rangle$ is inversely proportional to the diffusion constant: $D_s \propto \langle t_x \rangle^{-1}$, while $\langle t_p \rangle$ indicates the persistence time that a local structure would hold such that $\langle t_p \rangle \propto \eta/k_B T$. We can thus introduce a parameter

$$\lambda = \langle t_p \rangle / \langle t_x \rangle \propto \frac{D_s \eta}{k_B T} \quad (2)$$

to study the degree of DH for the system considered. For a system with DH, $D_s\eta$ is no longer a constant and this parameter λ would deviate from the value λ_0 given by SE relation. Therefore, we may use λ/λ_0 to characterize the degree of DH in this work.

One may note here that identifying DH with the violation of the SE relation might not be well justified in active fluids. This relation originates from a combination of the Stokes calculation (friction coefficient of a sphere in a Newtonian fluid) and Einstein's relation between the mobility and diffusion coefficients, which involves the temperature of the fluid. An active fluid is, in general, non-Newtonian and its macroscopic hydrodynamic equations are likely different from Navier-Stokes equations such that the very validity of the Stokes calculation is not certain. Moreover, for an active fluid it is, in general, far from obvious how to define temperature, and it is not clear whether there is a unique temperature [35,45–48]. Thus, the Einstein relation is not necessarily valid. Consequently, SE may not hold, in general, in active particles system. Nevertheless, investigation of λ/λ_0 as a function of the particle activity still helps us to understand DH behavior of the system.

C. Non-Gaussian parameter

For a system with DH, as mentioned above, structure relaxation and particle diffusion are spatially heterogeneous, with regions that are faster or slower than the average. One mainly observes that typical trajectories of a tagged particle, as shown in Fig. 1, are not smooth but rather composed of a succession of long periods of time where the particle simply vibrates within a small region, separated by random jumps. If one investigates the distribution of the particle displacements

at a given time, strong deviation from Gaussian distribution would be observed. Therefore, one may also characterize the DH of a system by such a deviation from Gaussian, which can be conveniently described by the so-called non-Gaussian parameter (NGP) $\alpha_2(\Delta t)$ defined as [49]

$$\alpha_2(\Delta t) = \frac{1}{2} \frac{\langle \Delta r^4 \rangle}{\langle \Delta r^2 \rangle^2} - 1, \quad (3)$$

where the factor $\frac{1}{2}$ corresponds to two-dimensional system. $\Delta r = |\mathbf{r}(t + \Delta t) - \mathbf{r}(t)|$ is the particle displacement for time lag Δt , wherein $\mathbf{r}(t) = (x(t), y(t))$ is particle position at time t . The angle brackets $\langle \dots \rangle$ here indicate an average over all particles and initial time t . If the particle undergoes normal diffusion homogeneously, the distributions of displacement $\Delta x = x(t + \Delta t) - x(t)$ and $\Delta y = y(t + \Delta t) - y(t)$ are of Gaussian type such that $\alpha_2(\Delta t) = 0$ by construction. If the distribution reveal tails and is much wider than expected for Gaussian, then $\alpha_2 > 0$, reflecting that there exists a population of particles that moves faster than the rest and appears to be more mobile, i.e., the system is dynamically heterogeneous at a time scale given by Δt . Hence, if the system gets phase separated wherein some particles are clustered together, one would expect that α_2 would be larger than zero. Generally speaking, the larger α_2 is, more heterogeneous the system is. If the displacement distribution is narrow but non-Gaussian, the values of α_2 may be negative. For instance, in the limiting case wherein all the particles move in the same direction homogeneously, the distribution would be a δ function such that $\langle \Delta r^4 \rangle = \langle \Delta r^2 \rangle^2$ and $\alpha_2 = -0.5$. Therefore, in our case, $\alpha_2 < 0$ generally indicates that a population of the particles performs cooperative directional motion due to the particle activity.

D. Four-point susceptibility

One can further understand the temporal DH behavior of a system by using the four-point susceptibility χ_4 which measures the correlation in dynamics between any two points in space within some time window [5,50,51]. Generally, χ_4 contains a self-part and a distinct part, reflecting the spatial correlations between temporarily localized particles and the correlated motion of particles into positions previously occupied by neighboring particles, respectively. In this work, we only compute the self-contribution part since it has been shown to be the dominating term [5]. By definition, this self-part is calculated from temporal fluctuations of the number of mobile particles, where a particle is defined to be mobile if its displacement over a time interval Δt is larger than some threshold value ΔL . At a given time t , one can then obtain the number of mobile particles $Q(t)$, which certainly changes from frame to frame with time. The self-part of χ_4 , which is evidently dependent on the choices of the time lag Δt and threshold length ΔL , is then computed from the temporal fluctuations of $Q(t)$ as [50]

$$\chi_4^s(\Delta t, \Delta L) = \frac{V}{N^2 k_B T} [\langle Q^2(t) \rangle_t - \langle Q(t) \rangle_t^2], \quad (4)$$

where $\langle \dots \rangle_t$ denotes averaging over time and superscript “s” denotes the self-part.

E. Vector correlation function

Note that χ_4 measures temporal fluctuations in mobility without regard for the spatial correlations between mobile particles, thus, it characterizes a type of temporal DH. Here, we further investigate the spatial DH of the system by using the vector spatial-temporal correlation function $S_{\text{vec}}(R, \Delta t)$ defined as [52]

$$S_{\text{vec}}(R, \Delta t) = \frac{\langle \Delta \vec{r}_i \cdot \Delta \vec{r}_j \rangle_{\text{pair}}}{\langle \Delta \vec{r}^2 \rangle}, \quad (5)$$

which characterizes correlations in the vector displacements $\Delta \vec{r}_i = \vec{r}_i(t + \Delta t) - \vec{r}_i(t)$ and $\Delta \vec{r}_j$ within time interval Δt . $\langle \dots \rangle_{\text{pair}}$ denotes an average over all particle pairs of which the initial distance is R and also over time t . The denominators of these correlation functions are averaged over all particles and thus not dependent on R . This correlation function would be unity if the particles are perfectly correlated and be zero for completely stochastic motions.

In the next section, we will present the results of λ/λ_0 , α_2 , χ_4 , and S_{vec} as functions of the particle activity characterized by τ , for different volume fractions φ_a . We have adopted event-driven Brownian dynamic (EDBD) approach to simulate Eqs. (1). The system parameters are number of particles $N = 10\,000$, $d = 0.4$, $v_0 = 10.0$, $D_0 = 0.05$ if not otherwise stated. The size of the simulation box is determined by the volume fraction. The SE value λ_0 is obtained by the simulation of a very dilute system consisting of passive particles, which is considered to be mostly homogeneous.

III. RESULTS AND DISCUSSIONS

In Fig. 2(a), the dependencies of λ/λ_0 as functions of τ are shown for different values of volume fraction φ_a . For the chosen parameter $D_0 = 0.05$, the SE value is $\lambda_0 \simeq 0.772$. Actually, we have found that λ_0 depends on D_0 very weakly, as demonstrated in the inset of Fig. 2. As can be seen, the effect of particle activity (τ) on the DH parameter (λ/λ_0) strongly depends on the volume fraction φ_a . For small volume fraction, say $\varphi_a = 0.3$, λ/λ_0 remains nearly 1 for relatively small τ , while it decreases to an apparently smaller value when τ gets larger. For $\varphi_a = 0.5$, λ/λ_0 is also nearly one for small τ , while it reaches a shallow valley at some intermediate value of τ , and then increases sharply to be apparently deviated from one. For an even larger volume fraction $\varphi_a = 0.7$, more interestingly, one observes a reentrance behavior: λ/λ_0 decreases from a value larger than one for small τ to a value approximately to be one for intermediate τ and then increases again for large τ . This interesting behavior had also been observed by Flenner *et al.* in Ref. [35], where the SE relation shows a nonmonotonic dependence on the persistence time of propulsion force.

The findings shown in Fig. 2(a) show rather nontrivial roles that particle activity plays on the DH behavior. To get more information, we have plotted the dependencies of $\langle t_p \rangle$ (dashed lines) and $\langle t_x \rangle$ (solid lines) on τ , respectively, in Fig. 2(b). Quite different features can be observed for different volume fractions. For $\varphi_a = 0.3$, both $\langle t_p \rangle$ and $\langle t_x \rangle$ decrease monotonically. If τ is small, $\langle t_p \rangle$ and $\langle t_x \rangle$ decrease simultaneously in a coherent way, such that $\lambda = \langle t_p \rangle / \langle t_x \rangle$ keeps nearly constant. If τ is large, one can see that $\langle t_p \rangle$ decreases a little faster than $\langle t_x \rangle$, leading to a decreasing

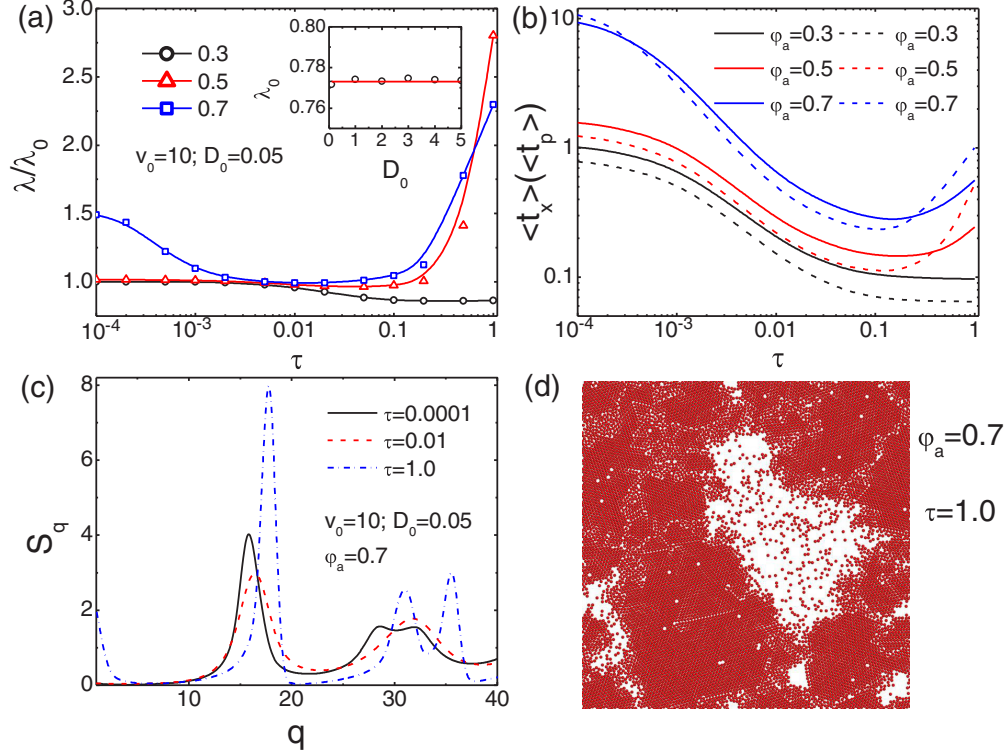


FIG. 2. (a) λ/λ_0 as functions of τ for different φ_a . Inset: λ_0 is nearly a constant with different fluctuation intensity. (b) Dependencies of $\langle t_p \rangle$ and $\langle t_x \rangle$ on τ . The solid and dashed-dotted lines correspond to $\langle t_x \rangle$ and $\langle t_p \rangle$, respectively. (c) Static structure factors S_q for $\varphi_a = 0.7$ with different τ . (d) Typical snapshot for $\tau = 1.0$ and $\varphi_a = 0.7$.

of λ/λ_0 with τ . For $\varphi_a = 0.5$, however, both $\langle t_p \rangle$ and $\langle t_x \rangle$ show a nonmonotonic dependence on τ , i.e., they both reach a minimum at some intermediate value of τ . In the range of large τ , $\langle t_p \rangle$ increases more sharply than $\langle t_x \rangle$, such that λ/λ_0 also increases sharply with τ as shown in Fig. 2(a). In the range of small τ , the situation is similar to that for $\varphi = 0.3$, i.e., $\langle t_p \rangle$ and $\langle t_x \rangle$ decrease in a coherent way such that λ/λ_0 remains nearly unchanged and the system is still dynamically homogeneous. For $\varphi_a = 0.7$, both $\langle t_p \rangle$ and $\langle t_x \rangle$ show nonmonotonically dependencies on τ , similar to the case for $\varphi_a = 0.5$. Nevertheless, in the range where τ is very small and the activity is weak, we observe a crossover of the values of $\langle t_p \rangle$ and $\langle t_x \rangle$ in correspondence with the reentrance behavior of λ/λ_0 for $\varphi_a = 0.7$ shown in Fig. 2(a).

The curves presented in Fig. 2(b) clearly show twofold roles of activity on the system's dynamics. If τ is small (weak activity), the main effect is to accelerate both the local structure relaxation and the diffusion, such that both $\langle t_p \rangle$ and $\langle t_x \rangle$ decrease. This is in coincidence with the picture that activity would lead to faster effective diffusion coefficient in the long time limit, which also corresponds to an effective temperature T_{eff} that is higher than the ambient temperature T [34]. In other words, the decreases of $\langle t_p \rangle$ and $\langle t_x \rangle$ with τ demonstrate that particle activity can “heat up” the system. On the other hand, if τ is large (strong activity), both $\langle t_p \rangle$ and $\langle t_x \rangle$ may increase for large volume fractions, indicating that both structure relaxation and particle diffusion slow down. This is consistent with another role of activity, which would induce effective attractive interaction [34] among the particles and lead to clustering or phase separation if the

volume fraction is large enough. The clustering of the particles would definitely lead to remarkable DH. In such a highly heterogeneous system, $\eta = \bar{\eta}_i$ and $D_s = \bar{D}_i$, wherein i denotes a cluster (or subdomain) that is homogeneous inside and the overbar denotes averaging over these clusters. While inside each cluster i one has $D_i \propto 1/\eta_i$, overall one would not expect $D_s \propto 1/\eta$ such that $D_s \eta \propto \langle t_p \rangle / \langle t_x \rangle$ would not be a constant. The average viscosity η is mainly contributed by those large clusters and it would increase sharply with largest cluster size. Nevertheless, the average diffusion coefficient D_s is mainly determined by those small clusters or fluid particles, and it would not decrease that fast as η increases. In a word, we believe that it is the dual role of particle activity, one is activity-induced higher effective temperature and the other is activity-induced clustering, that results in the reentrance behavior shown in Fig. 2(a) for large φ_a .

The above picture may be further elucidated by investigation of the static structure factor $S_q = \frac{1}{N} \langle \rho_{\mathbf{q}}(0) \rho_{-\mathbf{q}}(0) \rangle_{\text{NE}}$, where $\rho_{\mathbf{q}}(t) = \sum_i \exp[-i\mathbf{q} \cdot \mathbf{r}_i(t)]$ is the Fourier transform with vector \mathbf{q} of the collective particle density variable $\rho(\mathbf{r}, t) = \sum_i \delta(\mathbf{r} - \mathbf{r}_i)$. The subscript “NE” emphasizes that the averaging is performed when the system has reached the nonequilibrium steady state, rather than the equilibrium one. For an equilibrium system, S_q may be obtained by some analytical methods such as the Ornstein-Zernike (OZ) equation, however, the S_q^{NE} here must be obtained via direct simulations. Herein, we have calculated how S_q changes with τ for given volume fractions. Specifically, the results for $\varphi_a = 0.7$ are shown in Fig. 2(c). Note that for this large volume fraction, the system is already close to the glass

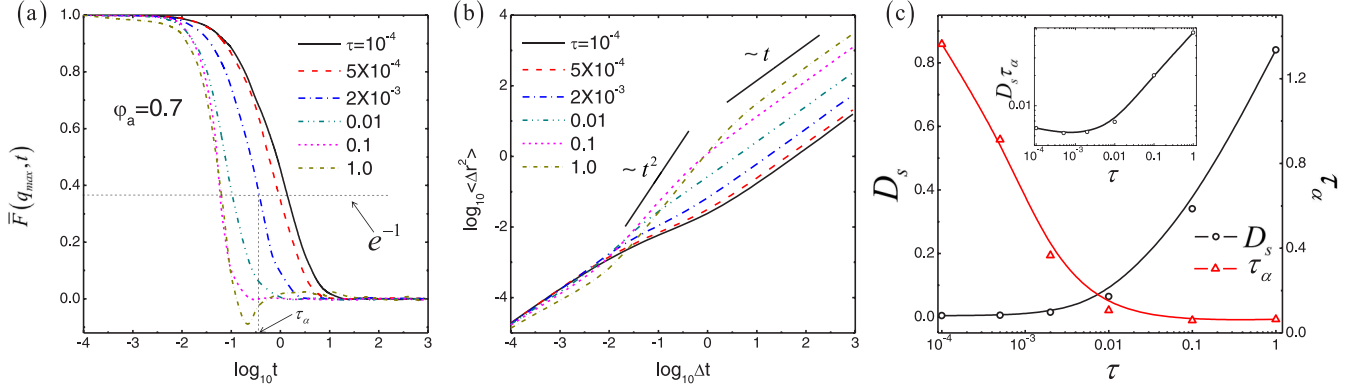


FIG. 3. (a) $\bar{F}(q_{\max}, t)$ vs t for different activity τ , where $q_{\max} = 15.2$ is the frequency position of first peak of S_q , t denotes the time interval. (b) The mean square displacement $\langle \Delta r^2 \rangle$ for different τ . (c) The long time diffusion coefficient D_s and structure relaxation time τ_α as functions of τ . Insets: the dependence of $D_s \tau_\alpha$ on τ .

transition, such that λ/λ_0 is deviated from the homogeneous value one even without activity or for very small τ . When τ increases from 10^{-4} to 0.01, one finds that the main peak of S_q decreases apparently and moves to a little bit larger value of q . This is consistent with the picture that activity tends to melt the system (a higher effective temperature) and the local structure becomes loosened. For much larger $\tau = 1.0$, however, we see that the main peak of S_q increases sharply and peak position shifts to a larger q , demonstrating the existence of strongly ordered local structures which is more compact. This is consistent with the second role played by particle activity, i.e., the particles become more strongly clustered. In addition, the value of S_q in the vicinity of $q \rightarrow 0$ tends to an apparent nonzero value, indicating large number fluctuations corresponding to phase separation. Figure 2(d) shows a typical snapshot for $\phi = 0.7$ and $\tau = 1.0$. Clearly, the system is phase separated into regular-structured clusters and a few random fluidlike particles.

As mentioned in Sec. II B, usually, the violation of SE is described by the deviation of the product $D_s \eta$ from a constant, with D_s the long time diffusion coefficient and η the viscosity. The analysis above has used an unusual way, namely, by calculating the parameter $\lambda = \langle t_p \rangle / \langle t_x \rangle$. To further demonstrate the violation of SE, it would be helpful to calculate $D_s \eta$ directly to see whether or not it shows a nonmonotonic dependence on the persistence time τ . The diffusion coefficient can be simulated directly by using the definition $D_s = \lim_{\Delta t \rightarrow \infty} \frac{\langle \Delta r^2 \rangle}{4\Delta t}$ for a two-dimensional system, wherein $\langle \Delta r^2 \rangle$ denotes the mean square displacement (MSD) in the time interval Δt . The viscosity η , however, is not convenient to calculate by simulation directly. Here, we adopt the same method as that in Ref. [13], wherein the authors used the fact that the viscosity η is proportional to the relaxation time τ_α of the local structure. Since the calculations of D_s and τ_α are rather time consuming, here we only show the data for $\phi_a = 0.7$ for illustration. In Fig. 3(a), the normalized collective scattering functions $\bar{F}(q, t) = N^{-1} \langle \rho_{\mathbf{q}}(t) \rho_{-\mathbf{q}}(0) \rangle_{\text{NE}} / S_q$ for $q = q_{\max} \simeq 15.2$ for different values of τ are shown. The dashed line indicates $\bar{F}(q_{\max}, t) = e^{-1}$, where the corresponding time in the horizontal axis defines τ_α . In Fig. 3(b), the MSDs as functions of time Δt are presented with the same set of τ as in Fig. 3(a), from which one can obtain the long time diffusion

coefficient D_s . Consequently, the dependencies of D_s and τ_α on τ are shown in Fig. 3(c), wherein D_s (τ_α) decreases (increases) monotonically with increasing τ , respectively. Comparing with Fig. 2(b), we do not observe nonmonotonic dependence of D_s or τ_α on the persistence time τ . Nevertheless, the product $D_s \tau_\alpha$ does show a minimum with the variation of τ , as demonstrated in the inset of Fig. 3(c), which is qualitatively consistent with the observation in Fig. 2(a).

In Fig. 4, we have presented α_2 as functions of time lag Δt for different activity τ and volume fraction ϕ_a . The results for small volume fraction $\phi_a = 0.3$ are depicted in Fig. 4(a). If the particle activity is small, e.g., $\tau = 10^{-4}$, α_2 is nearly zero for any Δt , indicating that the particles all undergo normal diffusions. For this small τ , the main effect is to enhance the system's effective temperature. With increasing activity τ , one can see that α_2 shows an apparent negative valley within an intermediate time range, after which α_2 becomes nearly zero again. As discussed in the last paragraph, the negative values of α_2 correspond to directional or superdiffusion behavior, and the width of the valley is basically identical to the range of time scale for superdiffusion. Clearly, the depth and width of the valley both increase with increasing τ , indicating more directional motion for larger activity as expected. For this small volume fraction, no obvious positive values of α_2 are observed such that the system is almost dynamically homogeneous, in accordance with the results reported in Fig. 2(a). In Fig. 4(d), we have also plotted the dependence of particle mean square displacement on time lag Δt for $\phi_a = 0.3$, corresponding to Fig. 4(a). Indeed, the particle exhibits normal diffusion (the slope of MSD with respect to Δt is larger than 1) in the intermediate time range for large values of τ , and the time range where it shows superdiffusion is in coincidence with those shown in Fig. 4(a) where α_2 shows apparent negative values. Therefore, for small volume fraction here, the main effect of large particle activity is leading to the cooperative directional motion of particles. This does make sense because τ actually corresponds to the persistence time of active particle to keep its original motion.

Nevertheless, the NGP α_2 in higher volume fractions such as $\phi_a = 0.5$ and 0.7 are considerably different from those shown in Fig. 4(a). For $\phi_a = 0.5$, the NGPs show dramatically

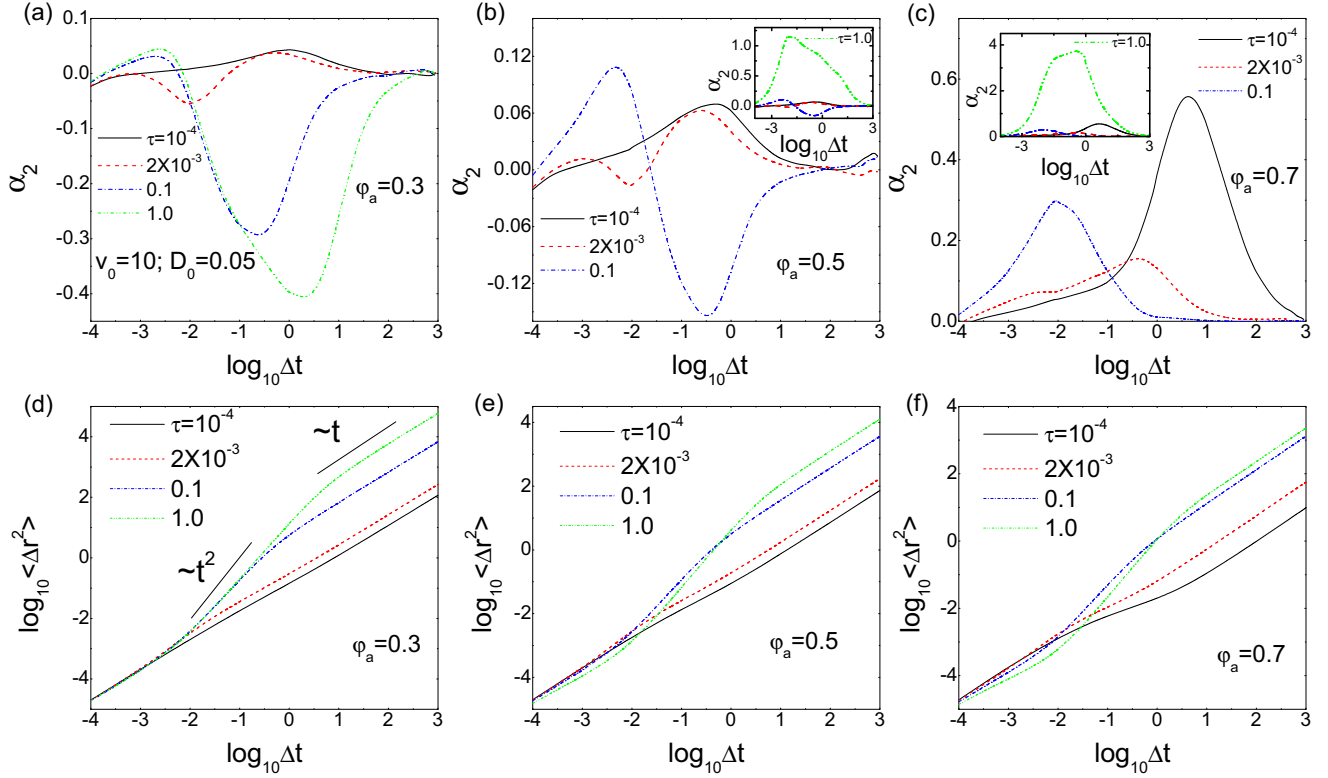


FIG. 4. Non-Gaussian parameter α_2 and mean square displacement $\langle \Delta r^2 \rangle$ vs Δt . The insets in (b) and (c) are the non-Gaussian parameters for $\tau = 1.0$. The driven velocity $v_0 = 10$ and fluctuation intensity $D_0 = 0.05$.

different behaviors for various activity. If the activity is small, say $\tau \lesssim 0.01$, the behavior is nearly the same as that in Fig. 4(a), i.e., α_2 does not show large deviation from zero in the whole time range. For a relatively larger $\tau = 0.1$, however, we observe a clear-cut positive peak in the short time range, demonstrating that the particles tend to aggregate within a short time range, in accordance with the effect of activity-induced clustering. Interestingly, these clusters are not that stable for $\phi_a = 0.5$, such that α_2 becomes negative again with increasing time Δt and the particles show superdiffusion again before they finally exhibit normal diffusion. This oscillating behavior of α_2 clearly demonstrates the competition between the two effects of particle activity: one is that leading to directional motion due to enhancement of persistence time τ , the other is the activity-induced clustering. Note that such a competition does not happen for $\phi_a = 0.3$ because activity-induced phase separation only takes place for volume fractions larger than a threshold value [28]. At short time scales, activity may lead to clustering due to effective negative pressure [31,33], while at long time run, particles may escape from the cluster if the persistence time τ is larger than the lifetime of the cluster. However, if the activity is strong enough, e.g., for $\tau = 1.0$, the clustering effect may dominate and it would keep stable, such that α_2 would be larger than zero for any time lag Δt , as shown in the inset of Fig. 4(b). The high peak of α_2 demonstrates that the system shows strong DH at this time scale. Correspondingly, the dependence of MSD on time Δt for $\phi_a = 0.5$ is plotted in Fig. 4(e). For small τ , the particles nearly show normal diffusions similar to that in Fig. 4(d). For $\tau = 0.1$ where α_2 oscillates, we observe a transition from normal to

superdiffusion at intermediate time range. For $\tau = 1.0$ where α_2 shows strong positive peak, the diffusion is slower than that for $\tau = 0.1$ in short time scale in accordance with the formation of stable large clusters. Interestingly, the particle also undergoes a superdiffusive behavior before it finally reaches normal diffusion in the long time limit, with a diffusion coefficient that is larger than that for $\tau = 0.1$.

For $\phi_a = 0.7$, which is close to the glass transition point, the system already shows obvious DH behavior even for small activity $\tau = 10^{-4}$. As shown in Fig. 4(c), α_2 shows a clear-cut positive peak at a relative large time scale. Correspondingly, the particle shows a subdiffusion behavior at this time scale as shown in Fig. 4(f), due to the cage effect in such a crowded environment. With a relative larger activity $\tau = 2 \times 10^{-3}$, the peak shifts to left with a lower peak, indicating a relatively less heterogeneous system. The particle still undergoes subdiffusion before it enters long time normal diffusion, as shown in Fig. 4(f). The shortening of the time scale for maximum α_2 and the decrease of the peak correspond to the melting role of activity, in accordance with the decrease of λ/λ_0 with τ in the small τ range shown in Fig. 2(a) for $\phi_a = 0.7$. With further increasing τ to 0.1, one still observes a shift of the α_2 peak to small time scale, while with an increase in the peak height. It seems that the system becomes more heterogeneous again with increasing τ , now on an even smaller time scale. Interestingly, the particle performs superdiffusion at this time scale [see Fig. 4(f)], where it changes from short time normal diffusion to long time normal diffusion. For an enough large $\tau = 1.0$, the peak of α_2 shifts back to longer time scales and the peak height becomes considerably high,

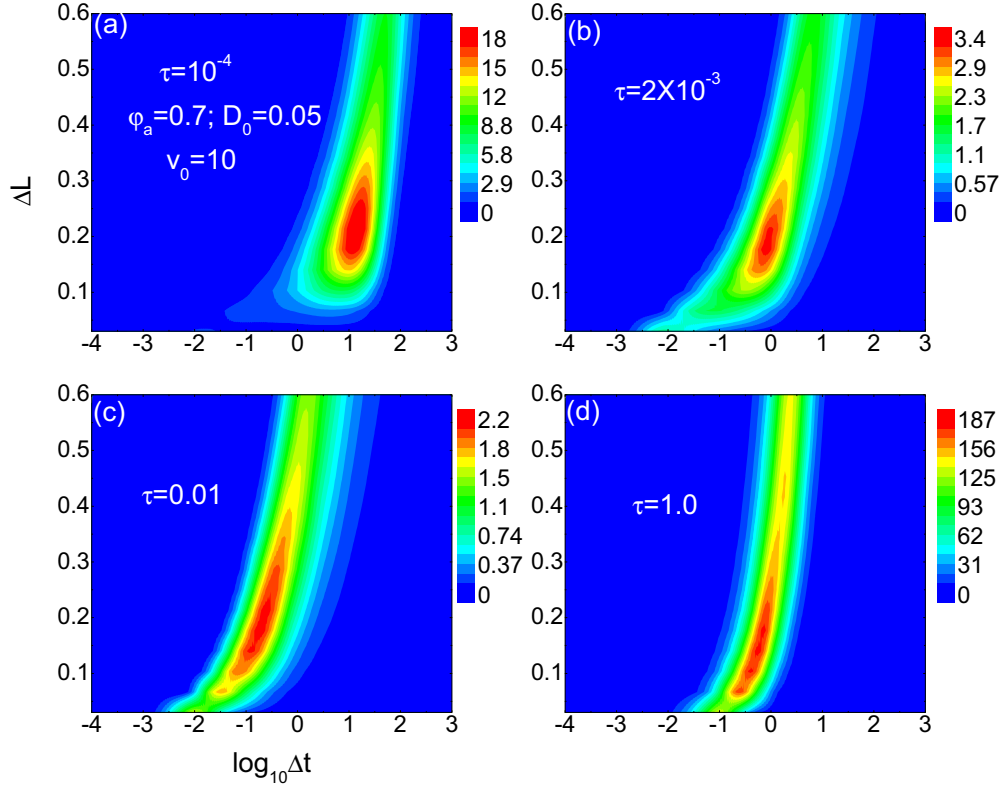


FIG. 5. Contour plot of χ_4^{ss} in the ΔL - $\log_{10} \Delta t$ plane. The same color in these figures corresponds to different values. (a) $\tau = 10^{-4}$, (b) $\tau = 0.002$, (c) $\tau = 0.01$, (d) $\tau = 1$. The red and blue colors correspond to maximum and minimum of χ_4 , respectively.

indicating strong heterogeneity. The short time diffusion is slow and a superdiffusion region is also present before the particle enters into long time normal diffusion. The increase of the α_2 peak again with increasing τ corresponds to the second role of particle activity that leads to clustering. Clearly, the variation tendency of α_2 with τ is consistent with the reentrance behavior of λ/λ_0 reported in Fig. 2(a) for $\varphi_a = 0.7$.

The above results already show that the system is dynamically heterogeneous for large volume fraction and activity apparently affects the degree of heterogeneity. In particular, for $\varphi_a = 0.7$, we observe a clear-cut nonmonotonic behavior where the degree of DH shows a minimum for an intermediate value of activity τ , via investigation of both the relative value λ/λ_0 or the NGP α_2 . We now try to further understand such a nontrivial observation from the temporal heterogeneity of the dynamics, by using the four-point susceptibility χ_4 . In Fig. 5, the contour plots of χ_4^s in the $(\Delta t, \Delta L)$ plane for $\varphi_a = 0.7$ are shown, with increasing activity τ from Figs. 5(a) to 5(d). The contour shows a characteristic maximum at $(\Delta t_{\max}, \Delta L_{\max})$ which indicates a typical time scale where the dynamics is most heterogeneous and a typical length scale distinguishing cage motions from cage rearrangements, respectively [5]. Generally, the peak value $\chi_{4,\max}^s$ quantifies the degree of temporal dynamic heterogeneity. From Fig. 5, one can see that $\chi_{4,\max}^s$ first decreases from an intermediate value (~ 18 for $\tau = 10^{-4}$) to a rather small one (~ 2.0 for $\tau = 0.01$), and then increases sharply to a considerably large value (~ 190 for $\tau = 1.0$). Such a nonmonotonic dependence of temporal heterogeneity on τ is fully consistent with the reentrance behavior shown in Fig. 2(a) for $\varphi_a = 0.7$. As discussed in

the related context there, small particle activity can liquefy the system and makes it homogeneous, while a large activity may lead to phase separation, again resulting in more considerable heterogeneity. The time scale Δt_{\max} , where the system is most heterogeneous, also shows a nonmonotonic dependence on τ : it first decreases and then increases. Such a dependence also demonstrates the dual role of particle activity: The peak first shifts to shorter time as τ increases due to the acceleration of particle directional motion, however, it reversely shifts to larger time due to the emergence of large stable clusters that slow down the motion. Note that the values of Δt_{\max} nearly coincide with the time scale where $\alpha_2(\Delta t)$ shows the maximum as shown in Fig. 4(c). As mentioned above, the maximum of α_2 occurs at the time scale where the particle jumps outside of local cages. It is reasonable that at this time scale, the number of mobile particles shows the largest fluctuation.

Note that χ_4 measures temporal fluctuations in mobility without regard for the spatial correlations between mobile particles, thus, it characterizes a type of temporal DH. Here, we further investigate the spatial DH for $\varphi_a = 0.7$ by using the vector spatial-temporal correlation function $S_{\text{vec}}(R, \Delta t)$. We fix the time lag $\Delta t = 1$, which is nearly Δt_{\max} for $\varphi_a = 0.7$ as shown in Fig. 5, and consider how S_{vec} changes with the initial distance R . The results are presented in Fig. 6 for different values of activity τ . Obviously, S_{vec} decreases monotonically with R for all values of τ , i.e., particles with larger initial distance R show less correlated motion after time lag Δt which is generally expected. For passive systems, it was reported [5] that S_{vec} is an exponentially decayed function of R , i.e., $S_{\text{vec}} \sim \exp(-R/\xi)$ where ξ denotes some type of length scale

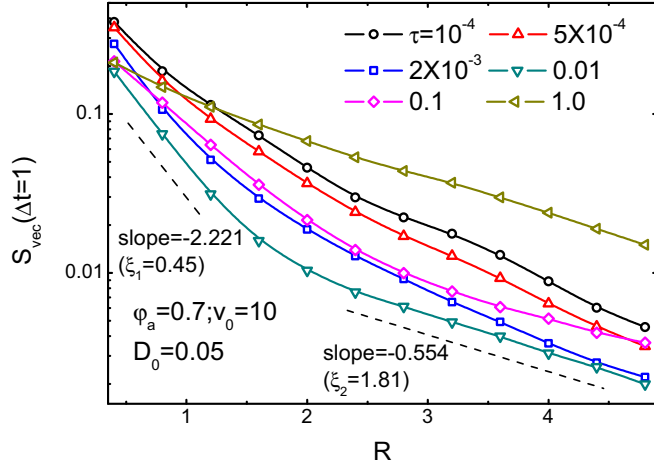


FIG. 6. S_{vec} as functions of distance R , where the time interval $\Delta t = 1$. The dashed lines are slopes of S_{vec} . $\xi_1 = 0.45$ and $\xi_2 = 1.81$ are two typical length scales in the system with $\tau = 0.01$.

for spatial correlation. For the active system considered here, however, the curves exhibit typical multiexponential characteristics (note that the left axis is in logarithmic scale), indicating that the system has more than one typical characteristic length scale. For instance, for $\tau = 0.01$, the curve can be approximately fitted by two joint straight lines as shown by the dashed lines. The inverses of the two slopes give the two typical length scales contained in the system, with $\xi_1 < \xi_2$. Interestingly, we also find a type of reentrance behavior with the increment of τ . When τ changes from a very small value 10^{-4} to a relatively larger one 0.01, one finds that the initial decay of S_{vec} with respect to R becomes sharper and the value of S_{vec} gets smaller, indicating that ξ_1 decreases and the correlation between neighboring particles becomes weaker, which is consistent with the picture that small activity tends to melt the system. With further increasing activity to 0.1, however, the curve goes up again with increasing correlation length scales. This latter effect is consistent with the second role of particle activity that leads to phase separation and stable clusters. It is interesting to note that for more larger activity, for instance $\tau = 1.0$, the curve can be well fitted by a single exponential decaying function again with a relative large correlation length. Such a single correlation length scale indicates that the system also shows a type of homogeneity or order, which is consistent with the pictures described in Figs. 2(c) and 2(d). Therefore, the correlation function S_{vec} also helps us to get more information about the system dynamics, here shown for $\phi_a = 0.7$.

Finally, we note that Fig. 2(a) also reveals another interesting reentrance behavior. For fixed activity $\tau = 1.0$, the value of λ/λ_0 for $\phi_a = 0.5$ is larger than both those for a smaller volume fraction $\phi_a = 0.3$ and that for a larger one $\phi_a = 0.7$. Generally, one may expect that a more crowded environment would be more heterogeneous due to cage effects. Therefore, such a nonmonotonic dependence of λ on the volume fraction ϕ_a is rather counterintuitive. To show more clearly, we have plotted λ/λ_0 as a function of ϕ_a for three different values of τ in Fig. 7. One can see that if activity τ is small, say $\tau = 10^{-4}$ or $\tau = 0.1$, λ increases monotonically with the volume fraction, indicating that the heterogeneity increases

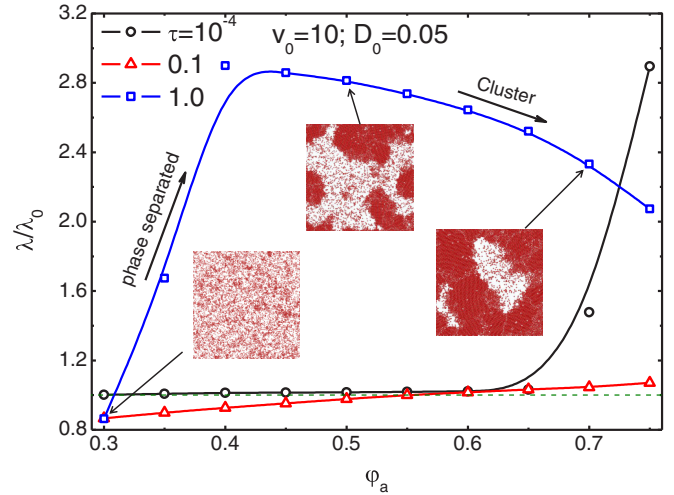


FIG. 7. λ/λ_0 via ϕ_a for different τ . Insets: typical snapshots for $\tau = 1.0$ and $\phi_a = 0.3, 0.5, 0.7$. The processes of phase separation and clustering are shown by the black arrows.

when the environment gets more crowded. However, for a large $\tau = 1.0$, λ undergoes a maximum at $\phi_a \simeq 0.45$ with the variation of ϕ_a , after which λ decreases apparently. In other words, if the activity is large enough, a more crowded system may become more dynamically homogeneous. To get more information, typical snapshots for $\phi_a = 0.3, 0.5, 0.7$ are shown in the insets of Fig. 7. As seen from these figures, the system clearly separates into two phases for $\phi_a = 0.5$, one solidlike and the other liquidlike. Since viscosity is dominated by the large solid clusters and diffusion is dominated by the small fluid particles, such a system would show strong heterogeneity. Nevertheless, for $\phi_a = 0.7$, although the system is more crowded, the particles aggregate together to form large solid clusters and few liquid particles exist. In a sense, the system is more like a single solid phase and thus more “homogeneous” compared to that for $\phi_a = 0.5$, such that the value of λ is smaller. To conclude, the activity-induced phase separation can, on one hand, increase the dynamic heterogeneity for small volume fractions and, on the other hand, can also lead to ordered cluster that becomes more like a single solid phase and decreases the dynamic heterogeneity.

One should note that when the system shows phase separation, for instance, for ϕ_a around 0.5 in Fig. 7, finite size effect may become non-negligible, which makes it necessary to run a large enough system in simulation. In a recent work [28], such an issue has been addressed by Redner *et al.* who compared the phase diagrams obtained by simulation and theory, finding that simulation results were fairly accurate for running the active systems with 15 000 particles. In our work, we have used 10^4 particles in simulations and we think that the finite size effect is not significant. What is more, the qualitative behavior that λ/λ_0 shows a nonmonotonic dependence on the volume fraction ϕ_a should be robust.

IV. CONCLUSION

In summary, we have investigated the influences of particle activity on the spatial and temporal DH of a system of active

hard-sphere particles. Each particle is subjected to an external driven force with constant amplitude, whereas its direction randomly changes via rotational diffusion with a correlation time τ , which can be used to characterize the particle activity. To obtain a systematic understanding, we have used a variety of observables to characterize the DH behavior, ranging from the violation of normal SE relation, the non-Gaussian parameter for particle displacement distribution, the four-point susceptibility to describe the temporal heterogeneity, as well as the vector spatiotemporal correlation function for spatial DH. We use a CTRW method to study the SE relation, by calculating the average waiting time $\langle t_x \rangle$ and the average persistence time $\langle t_p \rangle$, and investigating how the parameter $\lambda = \frac{\langle t_p \rangle}{\langle t_x \rangle}$ deviates from its SE value λ_0 . We show that λ/λ_0 depends strongly on the correlation time τ and volume fraction of particles φ_a . Interestingly, λ/λ_0 undergoes a minimum at an appropriate value of τ for large volume fraction φ_a , indicating that the most homogeneous dynamics would emerge for an optimal activity while stronger DH may be observed for both small and large activities. The non-Gaussian parameter $\alpha_2(\Delta t)$, four-point susceptibility $\chi_4(\Delta t)$, and vector spatiotemporal correlation $S_{\text{vec}}(\Delta t)$ have also been studied to further demonstrate and

illustrate this nontrivial reentrance behavior, showing that it is resulted from the competition between the dual roles of particle activity, namely, activity-induced higher effective temperature and activity-induced clustering. Moreover, λ/λ_0 also shows a maximum at an intermediate value of φ_a as well, indicating that less crowded system can be more heterogeneous than a more crowded one if the particle activity is large enough. Our work may shed new lights on the understanding of DH in nonequilibrium complex systems, which is of ubiquitous significance in soft matter and biological systems.

ACKNOWLEDGMENTS

This work is supported by National Basic Research Program of China (Grant No. 2013CB834606), by National Science Foundation of China (Grants No. 21521001, No. 21473165, and No. 21403204), by the Ministry of Science and Technology of China (Grant No. 2016YFA0400904), and by the Fundamental Research Funds for the Central Universities (Grants No. WK2060030018 and No. 2030020028,2340000074).

-
- [1] L. Berthier and G. Biroli, *Rev. Mod. Phys.* **83**, 587 (2011).
 - [2] W. Kob, C. Donati, S. J. Plimpton, P. H. Poole, and S. C. Glotzer, *Phys. Rev. Lett.* **79**, 2827 (1997).
 - [3] R. Yamamoto and A. Onuki, *Phys. Rev. E* **58**, 3515 (1998).
 - [4] M. D. Ediger, *Annu. Rev. Phys. Chem.* **51**, 99 (2000).
 - [5] T. Narumi, S. V. Franklin, K. W. Desmond, M. Tokuyama, and E. R. Weeks, *Soft Matter* **7**, 1472 (2011).
 - [6] Y. Rahmani, K. van der Vaart, B. van Dam, Z. Hu, V. Chikkadi, and P. Schall, *Soft Matter* **8**, 4264 (2012).
 - [7] T. E. Angelini, E. Hannezo, X. Trepast, M. Marquez, J. J. Fredberg, and D. A. Weitz, *Proc. Natl. Acad. Sci. USA* **108**, 4714 (2011).
 - [8] A. Heuer, M. Wilhelm, H. Zimmermann, and H. W. Spiess, *Phys. Rev. Lett.* **75**, 2851 (1995).
 - [9] M. T. Cicerone and M. D. Ediger, *J. Chem. Phys.* **103**, 5684 (1995).
 - [10] L. Berthier, *Phys. Rev. Lett.* **112**, 220602 (2014).
 - [11] P. Chaudhuri, L. Berthier, and W. Kob, *Phys. Rev. Lett.* **99**, 060604 (2007).
 - [12] R. Richert, *J. Phys.: Condens. Matter* **14**, R703 (2002).
 - [13] P. Kumar, S. V. Buldyrev, S. R. Becker, P. H. Poole, F. W. Starr, and H. E. Stanley, *Proc. Natl. Acad. Sci. USA* **104**, 9575 (2007).
 - [14] S.-H. Chong and W. Kob, *Phys. Rev. Lett.* **102**, 025702 (2009).
 - [15] K. V. Edmond, M. T. Elsesser, G. L. Hunter, D. J. Pine, and E. R. Weeks, *Proc. Natl. Acad. Sci. USA* **109**, 17891 (2012).
 - [16] U. Tracht, M. Wilhelm, A. Heuer, H. Feng, K. Schmidt-Rohr, and H. W. Spiess, *Phys. Rev. Lett.* **81**, 2727 (1998).
 - [17] M. Roos, K. Schäler, A. Seidlitz, T. Thurn-Albrecht, and K. Saalwächter, *Colloid Polym. Sci.* **292**, 1825 (2014).
 - [18] B. Schiener, R. Böhmer, A. Loidl, and R. V. Chamberlin, *Science* **274**, 752 (1996).
 - [19] T. Blochowicz and E. A. Rössler, *J. Chem. Phys.* **122**, 224511 (2005).
 - [20] R. Richert and S. Weinstein, *Phys. Rev. Lett.* **97**, 095703 (2006).
 - [21] M. T. Cicerone and M. D. Ediger, *J. Phys. Chem.* **97**, 10489 (1993).
 - [22] M. T. Cicerone and M. D. Ediger, *J. Non-Cryst. Solids* **407**, 324 (2015).
 - [23] J. Bosse, W. Götze, and M. Lücke, *Phys. Rev. A* **17**, 434 (1978).
 - [24] D. R. Reichman and P. Charbonneau, *J. Stat. Mech.* (2005) P05013.
 - [25] T. Vicsek and A. Zafeiris, *Phys. Rep.* **517**, 71 (2012).
 - [26] M. C. Marchetti, J. F. Joanny, S. Ramaswamy, T. B. Liverpool, J. Prost, M. Rao, and R. A. Simha, *Rev. Mod. Phys.* **85**, 1143 (2013).
 - [27] R. Ni, M. A. C. Stuart, and M. Dijkstra, *Nat. Commun.* **4**, 2704 (2013).
 - [28] G. S. Redner, M. F. Hagan, and A. Baskaran, *Phys. Rev. Lett.* **110**, 055701 (2013).
 - [29] H. Wioland, F. G. Woodhouse, J. Dunkel, J. O. Kessler, and R. E. Goldstein, *Phys. Rev. Lett.* **110**, 268102 (2013).
 - [30] E. Lushi, H. Wioland, and R. E. Goldstein, *Proc. Natl. Acad. Sci. USA* **111**, 9733 (2014).
 - [31] J. Stenhammar, R. Wittkowski, D. Marenduzzo, and M. E. Cates, *Phys. Rev. Lett.* **114**, 018301 (2015).
 - [32] R. Ni, M. A. Cohen Stuart, and P. G. Bolhuis, *Phys. Rev. Lett.* **114**, 018302 (2015).
 - [33] J. Bialké, J. T. Siebert, H. Löwen, and T. Speck, *Phys. Rev. Lett.* **115**, 098301 (2015).
 - [34] T. F. F. Farage, P. Krinninger, and J. M. Brader, *Phys. Rev. E* **91**, 042310 (2015).
 - [35] G. Szamel, E. Flenner, and L. Berthier, *Phys. Rev. E* **91**, 062304 (2015).
 - [36] G. Szamel, *Phys. Rev. E* **93**, 012603 (2016).
 - [37] V. Schaller, C. Weber, C. Semmrich, E. Frey, and A. R. Bausch, *Nature (London)* **467**, 73 (2010).

- [38] Y. Sumino, K. H. Nagai, Y. Shitaka, D. Tanaka, K. Yoshikawa, H. Chaté, and K. Oiwa, *Nature (London)* **483**, 448 (2012).
- [39] J. Schwarz-Linek, C. Valeriani, A. Cacciuto, M. E. Cates, D. Marenduzzo, A. N. Morozov, and W. C. K. Poon, *Proc. Natl. Acad. Sci. USA* **109**, 4052 (2012).
- [40] Y. Fily and M. C. Marchetti, *Phys. Rev. Lett.* **108**, 235702 (2012).
- [41] R. Wittkowski, A. Tiribocchi, J. Stenhammar, R. J. Allen, D. Marenduzzo, and M. E. Cates, *Nat. Commun.* **5**, 4351 (2014).
- [42] J. Palacci, C. Cottin-Bizonne, C. Ybert, and L. Bocquet, *Phys. Rev. Lett.* **105**, 088304 (2010).
- [43] E. Flenner, G. Szamel, and L. Berthier, *Soft Matter* **12**, 7136 (2016).
- [44] S. Pronk, E. Lindahl, and P. M. Kasson, *Nat. Commun.* **5**, 3034 (2014).
- [45] G. Szamel, *Phys. Rev. E* **90**, 012111 (2014).
- [46] D. Levis and L. Berthier, *Europhys. Lett.* **111**, 60006 (2015).
- [47] G. Szamel, *Europhys. Lett.* **117**, 50010 (2017).
- [48] Z. Preisler and M. Dijkstra, *Soft Matter* **12**, 6043 (2016).
- [49] P. Charbonneau, A. Ikeda, G. Parisi, and F. Zamponi, *Proc. Natl. Acad. Sci. USA* **109**, 13939 (2012).
- [50] S. C. Glotzer, V. N. Novikov, and T. B. Schröder, *J. Chem. Phys.* **112**, 509 (2000).
- [51] N. Lačević, F. W. Starr, T. B. Schröder, and S. C. Glotzer, *J. Chem. Phys.* **119**, 7372 (2003).
- [52] B. Doliwa and A. Heuer, *Phys. Rev. E* **61**, 6898 (2000).